

Diffusion of water in confined geometry: The case of a multilamellar bilayer

Marcello Sega and Renzo Vallauri*

CNR-INFM and Department of Physics, University of Trento, Via Sommarive 14, I-38050 Povo (Trento), Italy

Simone Melchionna

INFM —CRS SOFT, University of Rome “La Sapienza,” P.le A. Moro 2, I-00185 Rome, Italy

(Received 30 November 2004; revised manuscript received 10 June 2005; published 17 October 2005)

The diffusion of water confined in a stack of GM3 ganglioside bilayers is studied by computer simulation. A theoretical analysis of the behavior of the mean square displacement parallel and perpendicular to the bilayer surface is also provided in terms of diffusion equations in a very long time interval, between 2 ps and 2 ns. Such an analysis has allowed us to identify two different time regimes, to clarify the nature of nonlinear time dependence of the mean square displacement, and to give an interpretation to the origin of the often used time dependent diffusion coefficient. Both the effects of spatial inhomogeneities and boundary conditions are demonstrated to be the key points for the interpretation of all these results within a consistent theoretical framework.

DOI: [10.1103/PhysRevE.72.041201](https://doi.org/10.1103/PhysRevE.72.041201)

PACS number(s): 61.20.Ja, 82.70.Uv

In recent years the diffusion of liquids in confined geometries and inhomogeneous media has attracted the attention of many investigators [1–10]. It has been observed that in many physical situations the mean square displacement (MSD) of a single particle does not grow linearly in time, as predicted by the Brownian approximation in the long time regime. The onset of spatial and temporal correlations has in general been invoked to explain this phenomenon. The presence of such correlations has been commonly described either by introducing a phenomenological time-dependent diffusion coefficient $D(t)$ (see, for example, Ref. [11]), or by assuming that anomalous diffusion processes arise in presence of a corrugated surface, such that the MSD can be written as $|\mathbf{r}(t) - \mathbf{r}(0)|^2 = 6Dt^\alpha$ [8,9,12]. In particular this approach has been adopted to explain the diffusion of water in the proximity of a macromolecular surface [9]. However, it has also been argued that the effect of confinement alone, i.e., independent of the microscopic details of the confining medium, can explain the observed nonlinear time behavior of the MSD. Lindahl and Edholm [3] suggested that diffusion of water close to the surface of a protein (myoglobin), modeled as an infinite and sharp reflecting plane, leads to a nonlinear time dependence of the out-of-plane MSD. However, their statement has not been clearly substantiated by numerical experiments. In a recent paper Liu *et al.* have pointed out both the tensorial and local character of the diffusion coefficient and proposed a method to evaluate the diffusion tensor in presence of an interface [10]. While this appears to be a robust strategy to compute the diffusion tensor in inhomogeneous media, the authors restricted their analysis to the short time behavior of the MSD.

In this paper we report the results of a computer simulation study and theoretical analysis of the dynamics of water confined by an amphiphilic bilayer on previously unexplored time scales. From the data analysis, two interesting time re-

gimes appear, which are distinctly separated out. The theoretical analysis, performed along the lines suggested in previous works [3,10], is able to yield an unambiguous interpretation of the observed dynamical behavior, clarifying the relationship between the MSD nonlinearity and both spatial inhomogeneity and confinement.

We have used molecular dynamics to simulate a system composed by a bilayer of 128 GM3 gangliosides in presence of 6724 SPC water molecules and 128 Na^+ counterions. We have previously demonstrated that by employing a proper force field, the simulated system is representative of the real one, having examined in detail its structural properties in comparison with existing experimental data [13]. The system is simulated at atmospheric pressure and temperature of 333 K by means of the Berendsen thermostat and piston [14].

In Fig. 1 the density profile of the constituents across the

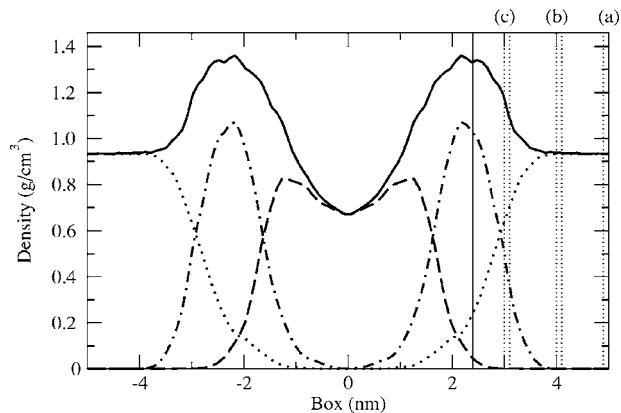


FIG. 1. Mass density profile of the simulated system (solid line), decomposed for different species, water (dotted line), lipid tails (dashed line), and saccharidic headgroups (dot-dashed line). The vertical dotted double lines (a), (b), and (c) indicate the initial position of water molecules whose MSD is detailed in Figs. 2, 3, and 5. The solid vertical line indicates the resulting position of the outer edge of the effective water layer.

*Electronic address: vallauri@science.unitn.it

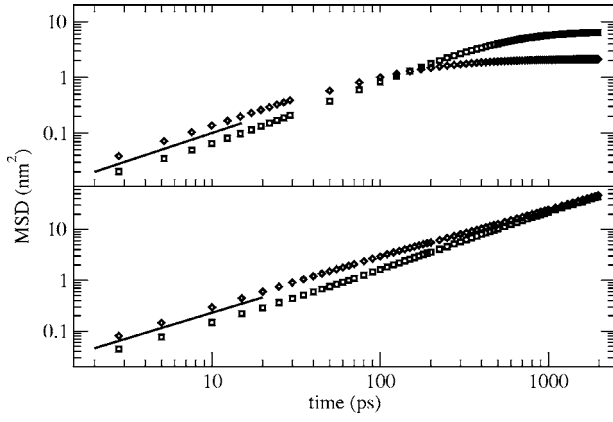


FIG. 2. MSD along the z direction (upper panel) and in the xy plane (lower panel) in the whole time range. Diamonds and squares refer to molecules starting from slabs (a) and (c), respectively. For comparison the linear time dependence is shown as a solid line.

bilayer is shown. Since periodic boundary conditions are imposed in all directions, the system represents a multilamellar bilayer with water confined between two neighboring lamellae. In such an inhomogeneous system it is natural to study separately the motion of water in the direction perpendicular (z direction) and parallel (xy plane) to the bilayer surface, as well as the dependence of the MSD from the initial position z_0 along the z axis.

We have evaluated the in-plane and out-of-plane MSD of molecules which at $t=0$ were located in slabs of thickness $\Delta z=0.1$ nm and at distance z_0 between 0 and 3 nm from the midpoint of the water layer. An overview of the full diffusive behavior is presented in Fig. 2 for two selected slabs. In all cases three distinct time scales can be identified; a short time regime ($t < 20$ ps), an intermediate regime ($20 < t < 500$ ps), and a long time span ($t > 500$ ps). The short time scale is characterized for both the in-plane and out-of-plane MSD by a linear behavior, that ends at the intermediate time region. In the third region the in-plane MSDs of molecules starting from different slabs converge to the same linear behavior, while the perpendicular MSD reaches plateau values dependent on the starting slab. The plateau is a mere consequence of confinement, so that the out-of-plane MSD has to lose the linearity at long times, differently from the case of unbounded media.

In view of the numerical results we propose the following interpretation of the MSD behavior in the whole explored time range. At first we write the diffusion equation for the probability density distribution $G(\mathbf{r}, t; z_0)$, choosing the appropriate boundary conditions to account for the presence of the bilayer, i.e., imposing $\partial G(\mathbf{r}, t; z_0)/\partial z=0$ at the bilayer surface. As shown later, these boundary conditions will play a role to obtain an approximate analytical solution for the MSD along the z direction, but the conclusions relative to the xy diffusion are not affected by this specific choice. Moreover, since the solvent is definitely inhomogeneous, showing considerable structure in the density profile, it is reasonable to introduce a diffusion tensor of diagonal form $\mathbf{D}(z) = \text{diag}(D_{\parallel}(z), D_{\parallel}(z), D_{\perp}(z))$, which depends on the distance from the bilayer, z . The complete diffusion equation then reads

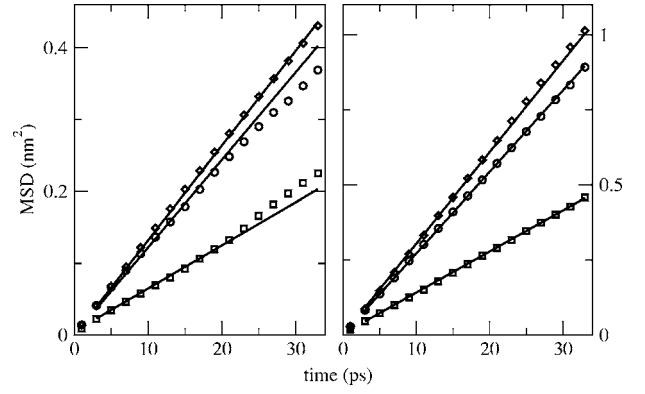


FIG. 3. Short time behavior of the out-of-plane (left panel) and in-plane MSD (right panel). Diamonds, circles, and squares refer to molecules starting from slabs (a), (b), and (c), respectively. The continuous lines represent the result of a linear fit in the interval 5–20 ps.

$$\partial_t G(\mathbf{r}, t; z_0) = \nabla \cdot [\mathbf{D}(z) \cdot \nabla G(\mathbf{r}, t; z_0)]. \quad (1)$$

Since the quantities of interest are computed by performing an average either on the xy plane or on the z direction, it is useful to introduce two reduced probability distributions, defined as $P_{\parallel}(x, y, t; z_0) = \int G(\mathbf{r}, t; z_0) dz$ and $P_{\perp}(z, t; z_0) = \int G(\mathbf{r}, t; z_0) dx dy$, so that the perpendicular MSD can be written as

$$\overline{|z(t) - z(0)|^2} = \int_0^{\ell} |z(t) - z(0)|^2 P_{\perp}(z, t; z_0) dz. \quad (2)$$

Here ℓ represents the effective width of the water layer. Integrating Eq. (1) on the z or xy domains, one derives the evolution equations for P_{\parallel} and P_{\perp} ,

$$\partial_t P_{\parallel}(x, y, t; z_0) = \left[\frac{\partial^2}{\partial x^2} + \frac{\partial^2}{\partial y^2} \right] \int_0^{\ell} D_{\parallel}(z) G(\mathbf{r}, t; z_0) dz, \quad (3)$$

$$\partial_t P_{\perp}(z, t; z_0) = \frac{\partial}{\partial z} \left[D_{\perp}(z) \frac{\partial}{\partial z} P_{\perp}(z, t; z_0) \right], \quad (4)$$

respectively. It is worth noticing that the equation for P_{\perp} is completely decoupled from the dynamics in the xy plane, whereas the time evolution for P_{\parallel} does indeed depend on the full probability density distribution $G(\mathbf{r}, t; z_0)$. However, in the two time regimes of short and long times, it is possible to decouple them, as we will soon see.

Let us start by examining the short time behavior. A linear fit performed in the range 5–20 ps shows a good agreement with the simulation data (see Fig. 3). Thus in this time interval the molecules undergo a standard Brownian motion with a diffusion coefficient dependent on the initial distance z_0 from the layer surface. This result is illustrated in Fig. 4, where the diffusion coefficient computed from the short time fit is presented. As apparent, molecules which are initially close to the surface diffuse about an order of magnitude less than those in the bulk, reflecting the strong interaction between water molecules and sugar groups in proximity of the

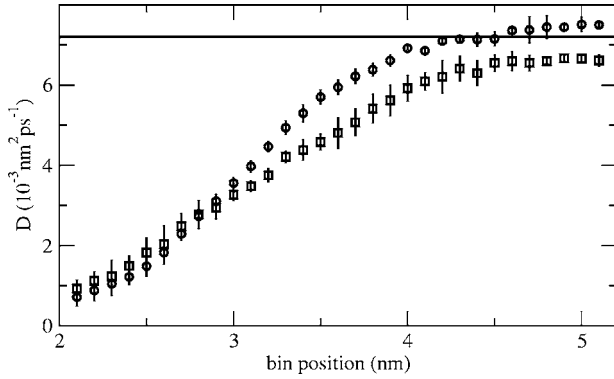


FIG. 4. Profile of the diffusion coefficient computed from the short time dependence of the MSD along the z direction (D_{\perp} , squares) and in the xy plane (D_{\parallel} , circles) with an estimate of an error bar. The solid horizontal line indicates the value of the diffusion coefficient of bulk SPC water at the same thermodynamic conditions.

ganglioside heads. Moreover, the difference between the in-plane and out-of-plane diffusion coefficients reflects the tensorial nature of this quantity.

The hypothesis of standard Brownian motion is valid for times short enough for Eqs. (3) and (4) to lead to a standard diffusion equation with $D_{\perp,\parallel}(z) \approx D_{\perp,\parallel}(z_0)$, i.e., constant along the spatial scale explored by the molecules. This approximation is valid for particles traveling distances shorter than $D_{\perp}/|\nabla D_{\perp}|$. Therefore the presence and extension of this linear regime strongly depends on the steepness of $D_{\perp}(z)$ and consequently on the degree of inhomogeneity. In the time interval 0–20 ps water molecules have traveled ~ 0.3 nm along the z direction, corresponding to about three slabs, and therefore experiencing a locally homogeneous environment. In addition, one can safely neglect the effect of boundary conditions for molecules not too close to the surface. Finally, it is worth remarking that the upper limit of what we have called the short time span (20 ps), is very often considered to be an asymptotic time regime [3,5,9].

Next, we show that Eqs. (3) and (4), which correctly describe the MSD in the short time span, are even very informative in the long time regime, when the effects of confinement and the spatial inhomogeneity produce the rich phenomenology seen in Fig. 2. At sufficiently long times the motion in the z and xy plane becomes uncorrelated, so that the distribution can be factorized as $G(\mathbf{r}, t; z_0) \approx P_{\parallel}(x, y, t; z_0)P_{\perp}(z, t; z_0)$. In this case we obtain

$$\partial_t P_{\parallel}(x, y, t; z_0) = \overline{D_{\parallel}(z_0, t)} \left(\frac{\partial^2}{\partial x^2} + \frac{\partial^2}{\partial y^2} \right) P_{\parallel}(x, y, t; z_0), \quad (5)$$

where

$$\overline{D_{\parallel}(z_0, t)} = \int_0^{\ell} D_{\parallel}(z) P_{\perp}(z, t; z_0) dz. \quad (6)$$

The main consequence of Eqs. (5) and (6) is that in the intermediate time regime the solution of Eq. (5) is a Gaussian with variance which does not grow linearly with time, as for the case of unbounded motion. Thus the in-plane MSD

deviates from the linear behavior (see Fig. 2, lower panel). Only at very long times P_{\perp} becomes stationary and, if particles are not trapped by the bilayer, the distribution does no longer depend on the starting point z_0 , and converges to the normalized water density profile along the z axis, $n(z)$. This is confirmed by the observation that all in-plane MSDs converge to the same slope (see Fig. 2, lower panel). Moreover, we can verify that at long enough times the distribution attains the stationary state by computing separately the two terms of the expression

$$\int_0^{\ell} D_{\parallel}(z) n(z) dz = \lim_{t \rightarrow \infty} \overline{D_{\parallel}(z_0, t)}, \quad (7)$$

where the left-hand side is the weighted integral of the diffusion coefficient computed at short times and the right-hand side is taken as a linear fit of the in-plane MSD at long times. The values obtained from the simulation data for the two members of Eq. (7) show an excellent agreement, being 5.7 and $5.6 \pm 0.1 \times 10^{-3} \text{ nm}^2 \text{ ps}^{-1}$, respectively. In addition, $\overline{D_{\parallel}(z_0, t)}$ can be now identified with the effective time dependent diffusion coefficient, since one can easily show that it is proportional to the time derivative of the in-plane MSD. This means that Eq. (6) provides an interpretation of the time dependent (in-plane) diffusion coefficient, which is usually introduced as a phenomenological parameter.

Let us now examine the long time diffusion along the z direction. Here the evolution equation does not produce any longer the standard Gaussian distribution since the diffusion coefficient depends on the z variable. Nevertheless, one can derive the limiting solution at long times by ignoring this dependence and substituting $D_{\perp}(z)$ with an effective parameter D . By retaining the reflecting boundary conditions, the diffusion equation can then be integrated (e.g., by variable separation [15]) to yield

$$P_{\perp}(z, t; z_0) = \frac{1}{\ell} + \sum_{n=1}^{\infty} \frac{2}{\ell} \exp\left[\frac{-D(\pi n)^2 t}{\ell^2} \right] \times \cos\left(\frac{\pi n z}{\ell} \right) \cos\left(\frac{\pi n z_0}{\ell} \right). \quad (8)$$

The corresponding MSD turns out to be

$$\overline{|z(t) - z_0|^2} = \frac{1}{3\ell} [(\ell - z_0)^3 + z_0^3] + \sum_{n=1}^{\infty} \frac{4\ell}{(n\pi)^2} \exp\left[\frac{-D(\pi n)^2 t}{\ell^2} \right] \times \cos\left(\frac{\pi n z_0}{\ell} \right) [z_0 + (\ell - z_0)(-1)^n]. \quad (9)$$

Since the water density profile does not go abruptly to zero at the bilayer surface, it is not obvious how to define the thickness ℓ of the diffusive region. However, an effective thickness can be estimated by noticing that at very long times the MSD for molecules starting from the center of the region ($z_0 = \ell/2$) reaches the asymptotic limit $\ell^2/12$. An effective thickness $\ell = 5.1$ nm can therefore be deduced from the simulation data. This value turns out to be compatible with the thickness of the water slab obtained from the density profile, as can be deduced from Fig. 1.

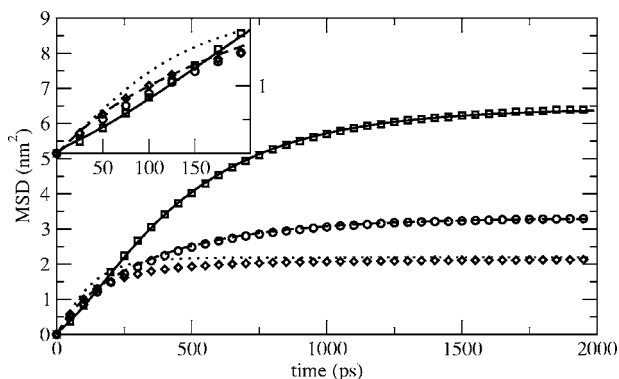


FIG. 5. MSD along the z direction for molecules starting from slab (a) (diamonds), (b) (circles), and (c) (squares). The lines represent the result of Eq. (9) with an effective parameter $D=6.5 \times 10^{-3} \text{ nm}^2 \text{ ps}^{-1}$. In the inset we compare the molecular dynamics data with the numerical solution in the intermediate time range.

The coefficient D introduced in Eqs. (8) and (9) plays the role of an effective parameter which the time scale over which $P_{\perp}(z, t; z_0)$ becomes uniform. By taking $D=6.5 \times 10^{-3} \text{ nm}^2/\text{ps}$ as an educated guess, we find a good agreement between the simulation results and Eq. (9) for all values of z_0 , as shown in Fig. 5.

Having set $D=\text{const}$, we do certainly neglect effects introduced by spatial inhomogeneities and the fact that the bilayer is not a perfectly reflecting medium. However, the good agreement reinforces the idea that geometrical constraints alone mostly capture the time evolution of the MSD in a wide temporal range. Interestingly, the solutions show

both a superlinear (Fig. 5, inset) and a sublinear behavior as often reported in the literature [9,16] thus accounting qualitatively for the observed time dependence of MSD. The fact that a single value for D allows a good fit of all curves, appears rather unexpected, in view of the large difference of the relative diffusion coefficients. However, in the time scale above 1 ns molecules have explored a very large portion of the available space so that the effect of spatial inhomogeneities appears to be unimportant.

In conclusion, we have shown that the investigation of time spans two order of magnitude longer than those usually considered, is of fundamental importance to attain a complete picture of diffusion in confined and inhomogeneous media. In particular we clearly demonstrated that (a) two different time regimes are present, at the time scale of 100 ps and 1 ns; (b) a simple Brownian model in an inhomogeneous medium—without any need for further hypotheses—predicts a nonlinear MSD as a consequence of both spatial inhomogeneity and confinement. This remains true even in case the probability distribution $G(\mathbf{r}, t)$ is factorized; (c) the often employed time dependent diffusion coefficient is more than a phenomenological parameter since it can be expressed as a weighted average of the local diffusion coefficient; (d) at very long times (≈ 1 ns) the in- and out-of-plane MSDs recover a standard diffusion behavior in an homogeneous medium, being $D_{\parallel}(z_0, \infty)$ and D the effective diffusion coefficients, respectively.

This work has been carried out under the FIRB project “Study of micro systems for controlled drug delivery,” financed by the Italian Ministry of Education. Computer resources from CINECA are kindly acknowledged.

-
- [1] M. H. J. Hagen, I. Pagonabarraga, C. P. Lowe, and D. Frenkel, *Phys. Rev. Lett.* **78**, 3785 (1997).
 [2] K. Åman, E. Lindahl, O. Edholm, P. Håkansson, and P.-O. Westlund, *Biophys. J.* **84**, 102 (2003).
 [3] E. Lindahl and O. Edholm, *Phys. Rev. E* **57**, 791 (1998).
 [4] S. Senapati and A. Chandra, *Chem. Phys.* **231**, 65 (1998).
 [5] V. A. Makarov, M. Feig, B. K. Andrews, and B. M. Pettitt, *J. Chem. Phys.* **75**, 150 (1998).
 [6] S. H. Lee and P. J. Rossky, *J. Chem. Phys.* **100**, 3334 (1994).
 [7] T. Róg, K. Murzyn, and M. Pasenkiewicz-Gierula, *Chem. Phys. Lett.* **352**, 323 (2002).
 [8] P. Gallo and M. Rovere, *J. Phys.: Condens. Matter* **15**, 7625 (2003).
 [9] A. R. Bizzarri and S. Cannistraro, *Phys. Rev. E* **53**, R3040 (1996).
 [10] P. Liu, E. Harder, and B. J. Berne, *J. Phys. Chem. B* **B108**, 6595 (2004).
 [11] I. Zuniga and P. Espanol, *Phys. Rev. Lett.* **71**, 3665 (1993).
 [12] R. Metzler and J. Klafter, *Phys. Rep.* **339**, 1 (2000).
 [13] M. Sega, P. Brocca, S. Melchionna, and R. Vallauri, *J. Phys. Chem. B* **108**, 20322 (2004).
 [14] H. J. C. Berendsen, J. P. M. Postma, A. DiNola, and J. R. Haak, *J. Chem. Phys.* **81**, 3684 (1984).
 [15] A. N. Tikhonov and A. A. Samarskii, *Equations of the Mathematical Physics* (Pergamon Press, Oxford, 1963).
 [16] S. G. Dastidar and C. Mukhopadhyay, *Phys. Rev. E* **68**, 021921 (2003).